The Effect of Solid Solutionizing Ti Element on Microstructural and Mechanical Properties of Extruded Cu-40Zn-Ti Ternary Alloy†

ATSUMI Haruhiko*, IMAI Hisashi, LI Shufeng**, KONDOH Katsuyoshi***, KOUSAKA Yoshiharu**** and KOJIMA Akimichi****

Abstract

The effects of solid solutionizing treatment and following hot extrusion on microstructural and mechanical properties of the extruded brass alloy (Cu-40Zn) with a small addition of titanium (Ti) were investigated in the present study. Cu-40Zn with 0.5 mass% Ti (Cu-40Zn-0.5Ti) alloy ingot was prepared by a casting process. This cast alloy consisted of α-β duplex phase structures. Furthermore, Cu-40Zn-0.5Ti alloy contained coarse Cu_2TiZn intermetallic compounds (IMCs) with 10-30 μm diameters. The IMCs were completely soluble in the both α and β phases by heat treatment at 973 K for 15 min. Cu-40Zn-0.5Ti alloy was pre-heated at 973 K for 15 min in solid solutionizing, and immediately extruded to fabricate a rod specimen of 7 mm diameter. The extruded specimen contained fine precipitates, having a mean particle sizes of 0.5 μm diameter, which were dispersed in both phases, not coarse Cu_2TiZn IMCs. In particular, since the grain growth of the α phase was inhibited by the pinning effect of the above fine precipitates at the grain boundaries, α phase consisted of fine grains. The extruded specimen consisted of remarkably fine and uniform α-β phases with an average grain size of 2.14 μm. The tensile properties of the extruded specimens showed an average value of yield strength: 304 MPa, ultimate tensile strength: 543 MPa, and 44 % elongation. The extruded specimens revealed suitable strengths and good ductility. The high strengthening mechanism of the wrought brass alloy was mainly due to the grain refinement of α and β phases by the fine precipitates derived from solid solutionizing Ti elements in the matrix.

KEY WORDS: (Brass), (Cu-40Zn), (Titanium), (Cu-40Zn-Ti), (High strength)

1. Introduction

Copper-Zinc alloys (Cu-Zn: brass) are widely used for lead frames, connectors and other electronic components, pipes, valves, and so on, because of their excellent electrical and thermal conductivities, corrosion resistance, good formability, and machinability. Furthermore, since brass alloys having α-β duplex phase structures (e.g. Cu-40mass%Zn alloy) reveal suitable strength and elongation[1-4], they have been applied for many industrial products. These alloys were also studied to improve their mechanical properties. For example, the commercial high-strength brass has been applied to marine propellers and bridge bearings because of high mechanical properties and corrosion resistance. This material is alloyed with Al, Mn, and Fe for solid solution strengthening and increasing area fraction of hard β-phases[5-7]. However, when the alloys are added with the larger amounts of metal elements, the coarser and brittle intermetallic compounds (IMCs) are produced in the matrix, and result in the drastic decrease of machinability[8-10]. Thus, brass alloys need to be strengthened by the small amounts of additives to decrease the content of such IMCs and disperse the fine IMCs in the matrix[11-13].

In this study, α-β duplex phase brass alloy with small addition of titanium (Ti) alloy was prepared by a casting process. Elemental Ti is alloyed into Cu as an additive for the improvement of its mechanical properties. Since an addition of elemental Ti is much effective for precipitation strengthening in Cu alloy, Cu-Ti alloys have been studied to achieve high strength and electrical conductivity as alternative materials to toxic Cu with Beryllium alloys[14, 15]. Moreover, the elemental Ti additive has been also the candidate for the improvement of the mechanical properties of brass alloys as previous reports[16, 17]. In the present study, the cast alloy was given a solid solutionizing treatment and a following hot extrusion in order to disperse the fine precipitates in the matrix. The effects of solid solutionizing and precipitates derived from elemental Ti additives on the

† Received on June 10, 2011
* Graduate Student
** Specially Appointed Researcher
*** Professor
**** San-Etsu Metal Co., Ltd.
Transactions of JWRI is published by Joining and Welding Research Institute, Osaka University, Ibaraki, Osaka 567-0047, Japan

microstructural and mechanical properties of the extruded brass alloy with α-β duplex phase were investigated.

2. Experimental

Cu-40mass%Zn alloy (Cu-40Zn: CAST1) and Cu-40Zn with addition of 0.5 mass% Ti alloy (Cu-40Zn-0.5Ti: CAST2) were prepared by casting processes. In detail, Cu-Ti alloy was melted at over 1673 K, and to the melt were added pure Zn at 1273 K, and then cast. The chemical compositions of brass cast ingots are shown in **Table 1**. The cast ingots of 60 mm diameter were machined into columnar billets of 41 mm diameter. They were hot-extruded by a 2000 kN hydraulic press machine (SHP-200-450: Shibayamakikai Co.) using an extrusion speed of 3 mm/s. Before extrusion, the billet was preheated at 923 K for 3 min and at 973 K for 15 min as solid solutionizing treatment condition in Ar gas atmosphere using a muffle furnace (KDF S-70: Denken Co.). The final diameter of extruded rods after extrusion was 7 mm. The two types of the extruded alloys were denoted as EXT923K and EXT973K. Microstructural observations were carried out by Optical microscope (OM, BX-51P: OLYMPUS) and SEM (JSM-6500F: JEOL). The microstructure of the cast and the extruded specimens was analyzed by SEM-EDS (EX-64175JMU: JEOL). For the electron back-scattered diffraction (EBSD) analysis, specimens with dimension 10×7×3 mm were cut parallel to the extrusion direction from extruded alloys. The specimens were ground with # 1000 and 4000 SiC abrasive papers, and then polished with 0.05 μm Al_2O_3 polishing suspension. Furthermore, they were electrochemical-polished in 30% HNO_3 methanol solution at 243K for 3 seconds, using a DC power supply with 30V. EBSD texture measurements were conducted by SEM, equipped with DigiView IV Detector (EDAX-TSL Co.) and OIM Data Collection 5.31 software (TSL Solutions K.K.). Tensile tests were carried out by using a universal testing machine (Autograph AG-X 50 kN: Shimadzu) with a strain rate of 5×10^{-4} /s. The extruded alloys were machined into tensile test specimens of 3 mm diameter in accordance with ICS 59.100.01.

Table 1 Chemical compositions of brass alloy cast ingots.

(mass%)	Pb	Ti	Zn	Cu
CAST1	-0.005	---	38.40	Bal.
CAST2	-0.005	0.496	38.96	Bal.

3. Results and discussion

Optical microstructures of CAST1 and CAST2 are shown in **Fig. 1**. Both of the cast specimens consisted of α-β duplex phase structures. The α-β duplex phase of both specimens showed similar morphology. The β-phase area fraction of CAST1 and CAST2 were 23 % and 47 %, respectively, which were calculated from image analyses of the optical microstructures. The grain size of the cast specimens was approximately over 100 μm. Furthermore, CAST2 specimens contained dispersoids of coarse IMCs having 10-30 μm diameters. **Table 2** shows the SEM-EDS analysis results of α-β phase and IMCs in cast alloys. The small amount of 0.09 ~ 0.16 at.% solute elemental Ti was detected in the α-β phase in CAST2. Since the content of solute Ti element in α-β phase was quite small, the almost all additions of elemental Ti existed as Cu_2TiZn IMCs in the cast ingot, which contained in 24 at.%Ti, 48 at.%Cu, and 28 at.%Zn as the almost similar compositions of Cu_2TiZn in a previous research[18].

Optical microstructures of the cast specimens, which were solid solutionizing treated at 973K for 15 min and following water-quenching are shown in **Fig. 2**. The area fraction of α-phase decreased by diffusion and phase transformations from α-phase to β-phase in each sample, when the solid solutionizing treatment was conducted at 973 K for 15 min. The β-phase fraction of CAST1 and CAST2 were 64 % and 89 %, respectively. On the other hand, Cu_2TiZn IMCs were never observed in CAST2 which were solid solutionized at 973 K for 15 min. The content of solid solutionizing Ti element in the β-phase increased from 0.13 at.% to 0.66 at.% revealed by SEM-EDS analysis, indicating the Cu_2TiZn IMCs were completely soluble in the matrix.

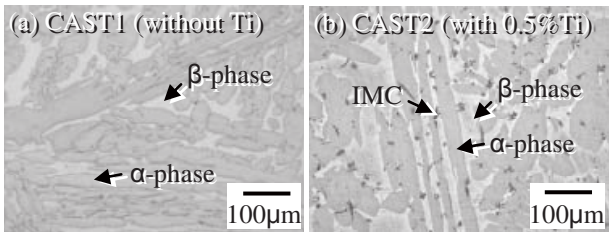

Fig. 1 Optical microstructures of brass alloy cast ingots: CAST1 (without Ti) (a) and CAST2 (with 0.5 mass%Ti) (b).

Table 2 Compositions of the α-β phase and the IMCs of CAST1 (without Ti) and CAST2 (with 0.5mass%Ti) acquired by SEM-EDS point analysis.

		Elements (at.%)		
		Ti	Cu	Zn
CAST1	α	---	64.72	35.28
	β	---	57.21	42.79
CAST2	α	0.12	65.4	34.48
	β	0.13	57.58	42.29
	IMC	24.16	47.59	28.25

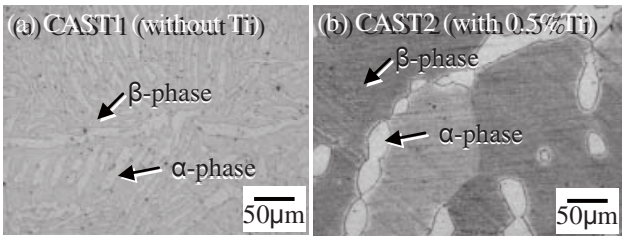

Fig. 2 Optical microstructures of solid solutionizing specimens at 973 K for 15 min: CAST1 (a) and CAST2 (b).

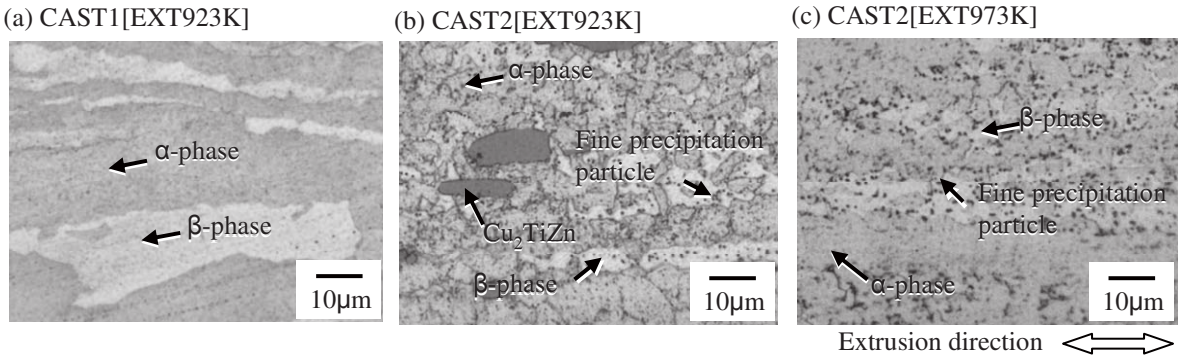

Fig. 3 Optical microstructures of extruded specimens pre-heated at 923 K for 3 min; CAST1[EXT923K] (a) and CAST2[EXT923K] (b), and at 973 K for 15 min; CAST2[EXT973K] (c).

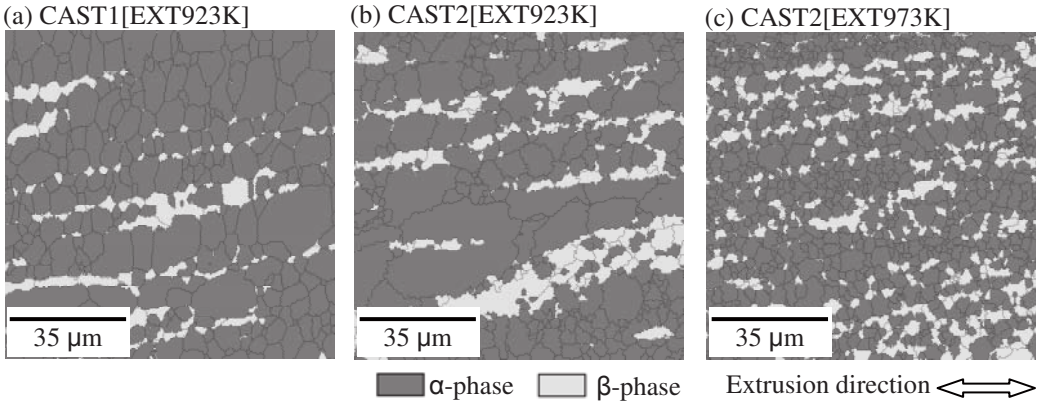

Fig. 4 Grain distribution of the α-β duplex phase structures of CAST1[EXT923K] (a), CAST2[EXT923K] (b), and CAST2[EXT973K] (c) by EBSD analysis.

Figure 3 indicates optical microstructures of the extruded alloys denoted as EXT923K and EXT973K on the parallel cross-section of the extrusion direction. When cast alloys were extruded, CAST1[EXT923K] and CAST2[EXT923K] specimens were pre-heated at 923 K for 3 min and CAST2[EXT973K] was pre-heated at 973 K for 15 min in the solid solutionizing treatment condition. The α-β duplex phase structures of the extruded specimens were observed to be slightly elongated along the extrusion direction in each extruded alloy. Their detailed grain distribution will be mentioned later. Furthermore, the coarse Cu_2TiZn IMCs were dispersed in the matrix of CAST2[EXT923K] as the same results in observation of CAST2 specimens as shown in Fig. 1 (b). A small amount of fine precipitation particles with 0.5 μm in diameter were also dispersed in the matrix of CAST2[EXT923K]. On the other hand, instead of coarse Cu_2TiZn IMCs, the fine precipitation particles were densely distributed in the α-β duplex phase matrix of CAST2[EXT973K] as shown in Fig. 3 (c). In the case of CAST2[EXT973K], since coarse Cu_2TiZn IMCs were completely soluble in the matrix during pre-heating the billets at 973 K for 15 min before extrusion as shown in Fig. 2 (b), these fine particles observed in the matrix were precipitated from solid solutionizing Ti element in α-β phase during cooling after the extrusion.

Figure 4 and **Table 3** show the grain distribution, and the area fraction and average grain size of α-β duplex phase structures on EXT923K and EXT973K in the parallel cross-section of the extrusion direction revealed by EBSD analysis. CAST2[EXT973K] had finer and more uniform α-β duplex phase structures compared with CAST1[EXT923K] and CAST2[EXT923K]. In particular, the average α-phase grain size of CAST2[EXT973K] was 2.15 μm, which was 44 % finer than that of CAST2[EXT923K] which contained the coarse Cu_2TiZn IMCs. It is considered that the CAST2 specimen was characterized by a larger area fraction of β-phase at the extrusion condition of 973 K for 15 min as shown in Fig. 2 (b), compared with that of the CAST2 specimen at the room temperature as shown in Fig. 1 (a). This is due to the nucleation of fine α-phase from β-phase during cooling after the extrusion[19], and the α phase grain growth was inhibited by the pinning effect of the fine precipitation particles at the grain boundaries as shown in Fig. 3 (c). Since CAST2[EXT923K] had not enough fine precipitates in the matrix, it revealed a similar grain size of α-β phase (3.51 μm) compared with that of CAST1[EXT923K] (3.89 μm). When the Cu-40Zn with elemental Ti alloys were pre-heated at high temperature and then extruded, their α-β phase grains were refined during the dynamic recrystallization and phase transformation by the fine precipitates which were derived from the solid solutionizing Ti element. On the

other hand, the area fraction of hard β-phase to the matrix indicated similar values in each extruded specimen as shown in Table 3.

Tensile stress-strain curves of EXT923K and EXT973K specimens are shown in **Fig. 5**. The yield strength (YS) and the ultimate tensile strength (UTS) of CAST2[EXT923K] were 226 MPa and 519 MPa, respectively. The YS of CAST2[EXT923K] was comparable with that of extruded CAST1[EXT923K] (224 MPa) with no additives. This is because the extruded CAST1[EXT923K] specimen had an average grain size of 3.89 μm and area fraction of α:β = 84:16, at the almost similar level of CAST2[EXT923K] as shown in Table 3. The YS of the extruded specimens were determined by the balance between grain size and area fraction of α and β-phase. On the other hand, although, in the case of α-β duplex phase brass, their YS and UTS decreased with increasing the extrusion temperature [19], the YS and UTS of CAST2[EXT973K] were 304 MPa and 543 MPa, respectively, which were 35 % and 4 % higher than that of CAST2[EXT923K]. Particularly, this is because the increment of YS was due to the grain refinement strengthening as shown in Fig. 4 (c). The strengthening $\Delta\sigma_y$ was calculated by the following Hall-Petch equation

$$\Delta\sigma_y = k \times (d_{EXT973K}^{-1/2} - d_{EXT923K}^{-1/2})$$

where k is Hall-Petch coefficient: 528 N/μm$^{3/2}$ [20], in the case of Cu-40Zn-Ti alloy, $d_{EXT973K}$ and $d_{EXT923K}$ are average grain diameter 2.14 μm and 3.51 μm, respectively, as shown in Table 3. The calculated $\Delta\sigma_y$ was 79 MPa by the above Hall-Petch equation. This value was similar to the experimental increment value of YS (78 MPa). Furthermore, since CAST2[EXT923K] and CAST2[EXT973K] had also a similar levels of the area fraction of between α and β-phase, the main strengthening mechanism of extruded specimens in different thermo-mechanical treatment conditions was grain refinement strengthening.

On the other hand, since the elongation of CAST2[EXT973K] specimens had also an average value of 44 %, which was as well as that of CAST2[EXT923K] (46 %), The drastic deterioration of elongation never occurred by the strengthening as previously mentioned. The elongation of CAST2[EXT923K] specimens were decreased by the coarse Cu_2TiZn IMCs, compared with that of CAST1[EXT923K] (51 %). In the case of extruded wrought brass alloy without any additives, the hot extrusion temperature (ranging from 923 K to 1023 K) had no effect on the elongation of the extruded brass alloy in tensile tests [19]; thus, the elongation improvement of CAST2[EXT973K] was due to the fine precipitates in the matrix, instead of coarse Cu_2TiZn IMCs as shown in Fig. 3 (c). SEM observations of the fractured surface of the tensile test specimen of CAST2[EXT923K] and CAST2[EXT973K] are shown in **Fig. 6**. Fine and uniform dimples were observed on the fractured surface of CAST2[EXT973K] due to the fine α-β duplex phase structures as previously mentioned. On the other hand, some coarse particles with brittle surfaces distributing in the center of large dimples were observed on the fractured surface of CAST2[EXT923K]. These brittle fractured surface areas were identified as Cu_2TiZn IMCs by SEM-EDS analysis, as shown in Fig. 3 (b). Such coarse Cu_2TiZn IMCs caused a decrease of the elongation of wrought brass alloys. As a result, CAST2[EXT973K] without coarse Cu_2TiZn IMCs revealed the excellent strength and ductility.

Table 3 Microstructural characteristics of CAST1[EXT923K], CAST2[EXT923K], and CAST2[EXT973K] obtained by EBSD analysis.

		α	β	α-β
CAST1 EXT923K	Area fraction (%)	84	16	---
	Grain size /μm	4.51	2.57	3.89
CAST2 EXT923K	Area fraction (%)	80	20	---
	Grain size /μm	3.83	2.64	3.51
CAST2 EXT973K	Area fraction (%)	79	21	---
	Grain size /μm	2.15	2.10	2.14

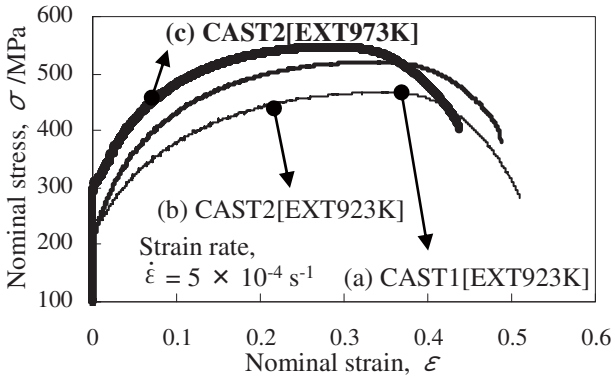

Fig. 5 Stress-strain curves of CAST1[EXT923K] (a), CAST2[EXT923K] (b), and CAST2[EXT973K] (c) in tensile.

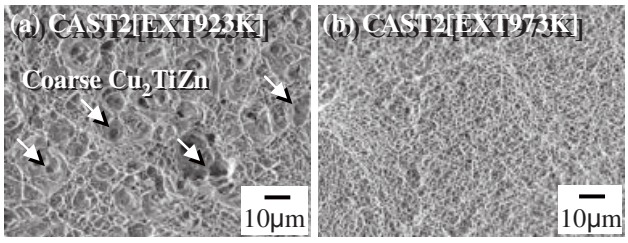

Fig. 6 SEM observation of fractured surface of the tensile test specimens of CAST2[EXT923K] (a) and CAST2[EXT973K] (b).

4. Conclusions

In this study, the microstructural and mechanical properties of the Cu-40Zn-0.5Ti ternary alloys via solid solutionization and the following extrusion were investigated. The extruded specimen which was pre-heated at 973 K for 15 min and then extruded consisted of fine and uniform α-β duplex phase structures having an average grain size of 2.14 μm in diameter. Furthermore, the fine precipitates with a mean particle sizes of 0.5 μm diameter were densely dispersed in the matrix, resulting from the precipitation of the solid solutionizing Ti element. Particularly, α-phase consisted of fine grains due to the pinning effect by the fine precipitates at the grain boundaries. The tensile test results indicated YS: 304 MPa, UTS: 543 MPa and 44 % elongation. The high strengthening mechanism of the wrought brass alloy was mainly due to the grain refinement of α and β phases by the pinning effect of the fine precipitates.

Acknowledgement

Nippon Atomized Metal Powders Corporation is acknowledged for their help with preparing the brass cast ingots used in this study.

References

1) V. Randle, H. Davies, Evolution of Microstructure and Properties in Alpha-Brass after Iterative Processing, Metallurgical and Materials Transactions A, 33 (2002) 1853-1856.
2) G. Pantazopoulos, Leaded Brass Rods C 38500 for Automatic Machining Operations: A Technical Report, Journal of Materials Engineering and Performance, 11 (2002) 402-407.
3) J. X. Wu, M. R. Ji, M. Galeotti, A. M. Giusti and G. Rovida, Surface Composition of Machined Leaded Brass, Surface and Interface Analysis, 22 (1994) 323-326.
4) H. Imai, Y. Kosaka, A. Kojima, S. Li, K. Kondoh, J. Umeda, H. Atsumi, Characteristics and machinability of lead-free P/M Cu60–Zn40 brass alloys dispersed with graphite, Powder Technology, 198 (2010) 417-421.
5) U. Borggren, M. Selleby, A Thermodynamic Database for Special Brass, Journal of Phase Equilibria, 24 (2003) 110-121.
6) H. Mindivan, H. Çimenoˇglu, E.S. Kayali, Microstructures and wear properties of brass synchroniser rings, Wear, 254 (2003) 532-537.
7) M. Sundberg, R. Sundberg, S. Hogmark, R. Otterbergc , B. Lehtinenc, S. E. Hgrnstrgm, S. E. Karlsson, Metallographic Aspects on Wear of Special Brass, Wear, 115 (1987) 151-165.
8) G. Mauvoisin, O. Bartier, R. El Abdi, A. Nayebi, Influence of material properties on the drilling thrust to hardness ratio, International Journal of Machine Tools & Manufacture, 43 (2003) 825-832.
9) C. Vilarinho, J.P. Davim, D. Soares, F. Castro, J. Barbosa, Influence of the chemical composition on the machinability of brasses, Journal of Materials Processing Technology, 170 (2005) 441-447.
10) L. Z. Jin, R. Sandstrm, Machinability data applied to materials selection, Materials & Design, 15 (1994) 339-346.
11) H. Atsumi, H. Imai, S. Li, Y. Kousaka, A. Kojima, K. Kondoh, Microstructure and Mechanical Properties of High Strength Brass Alloy with Some Elements, Materials Science Forum, 654 - 656 (2010) 2552-2555.
12) S. Li, H. Imai, H. Atsumi, K. Kondoh, Characteristics of high strength extruded BS40CrFeSn alloy prepared by spark plasma sintering and hot pressing, Journal of Alloys and Compounds, 493 (2010) 128-133.
13) S. Ikeno, K. Matusda, Y. Nakamura, T. Kawabata, Y. Uetani, TEM Observation of α-phase in 60/40 Brass with Additional Element of Si, Mg or Ni, Jounal of the JIRICu, 43 (2004) 26-30.
14) W.A. Soffa, D.E. Laughlin, High-strength age hardening copper–titanium alloys: redivivus, Progress in Materials Science, 49 (2004) 347–366.
15) S. Nagarjuna, M. Srinivas, K. Balasubramanian, D. S. Sarma, The Alloy Content and Grain Size Dependence of Flow Stress in Cu-Ti Alloys, Acta Materialia, 44 (1996) 2285-2293.
16) S. Li, H. Imai, H. Atsumi, K. Kondoh, Contribution of Ti addition to characteristics of extruded Cu40Zn brass alloy prepared by powder metallurgy, Materials and Design, 32 (2011) 192-197.
17) S. Li, K. Kondoh, H. Imai, H. Atsumi, Fabrication and properties of lead-free machinable brass with Ti additive by powder metallurgy, Powder Technology, 205 (2011) 242–249.
18) D. Soares, C. Vilarinho, F. Castr, Contribution to the knowledge of the Cu-Zn-Ti system for compositions close to brass alloys, Scandinavian Journal of Metallurgy, 30 (2001) 254–257.
19) C. Mapelli, R. Venturini, Dependence of the mechanical properties of an a/b brass on the microstructural features induced by hot extrusion, Scripta Materialia, 54 (2006) 1169–1173.
20) E. Werner, H. P. Stijwe, Phase Boundaries as Obstacles to Dislocation Motion, Materials Science and Engineering, 68 (1984-1985) 175-182.